The Effects of Helical Ribs' Number and Grid Types on the Buckling of Thin-walled GFRP-stiffened Shells under Axial Loading

M. YAZDANI* AND G. H. RAHIMI
Department of Mechanical Engineering, Tarbiat Modares University
P O Box 14115-143, Tehran, Iran

ABSTRACT: The results of an experimental study on the buckling behavior of thin-walled GFRP-stiffened cylindrical shells are presented. The buckling behavior of stiffened shells, with lozenge and triangular grids, and unstiffened shells were studied under quasi-static axial loading at room temperature. The effect of the number of helical ribs and grid shapes was thoroughly investigated. During the experimental study, local skin buckling mode was observed on all specimens. Based on the findings from this work, a minimum number of stiffeners should be present in a structure in order to play an effective role in its strength. Furthermore, it was concluded that under axial loading, increasing the number of helical ribs is more effective than adding hoop rings and changing the grid types.

KEY WORDS: buckling load, specific load, composite shells, stiffened shells.

INTRODUCTION

STRUCTURAL EFFICIENCY IS a major concern in today's aerospace applications. One of the most famous structures in this regard is the grid-stiffened composite cylindrical shell. This has certain kinds of stiffening structures either on the inner, outer, or both sides of the shell. These types of composite shells have a high buckling capacity together with lower mass compared to metal shells. Up till now, there is no published research in the open literature on the effects of grid parameters on the failure behavior of the stiffened shells using an experimental approach. An experimental study was conducted by Baker and Bennett on the buckling of nuclear containment like cylindrical geometries under combined shear and bending [1]. They developed a method for determining the static buckling interaction curves of both ring-stiffened and unstiffened cylindrical geometries. Fabrication and testing of thin composite isogrid-stiffened shells and panels were described by Kim [2,3]. In these papers, the fabrication and axial compression testing of composite isogrid-stiffened shells and panels were discussed. The buckling load of CFRP unstiffened composite cylinders under combined axial and torsional loadings was investigated by Meyer-Piening [4]. The aim of this study was to determine the buckling load of

*Author to whom correspondence should be addressed. E-mail: myazdani@sut.ac.ir
Figures 1–6 appear in color online: http://jrp.sagepub.com

0731-6844/10/17 2568–8 $10.00/0 DOI: 10.1177/0731684409355202

unstiffened cylindrical shells with different laminate lay-ups. Several shells were tested under axial compression and also under combined axial compression and superimposed torsion. It was found that the stiffness eccentricity of the laminate plays a significant role on the magnitude of the axial buckling load, while this effect is somewhat marginal for combined loads.

Bisagni and cordisco conducted an experimental study on the buckling and post-buckling behaviors of four unstiffened thin-walled CFRP cylindrical shells [5], where the test equipment used was able to apply axial and torsional loadings separately, or in combination. The results identified the effect of laminate orientation, and showed that the buckling loads were essentially independent of load sequence, and the shells were able to sustain load in the post-buckling field without any damage. Kidane and Wodesenbet computed the buckling load of grid-stiffened composite cylinders by using the smeared method and classical lamination theory [6,7]. They compared the obtained results to those from the experimental and the finite element methods. Post-buckling and collapse experiments of the stiffened composite cylindrical shells subjected to axial and torque loadings were carried out by Bisagni and cordisco [8]. The buckling and post-buckling tests were performed until the collapse of the three stiffened composite cylindrical shells. The shells, different in the skins and in the stiffeners lay-up, were expressly designed for working in the post-buckling field. The strength capacity of these structures to work in the post-buckling range was determined. All specimens had only longitudinal metallic stiffeners, which were joined to the outer shell by bolts, so none of them were fully composite-stiffened shells. Yazdani et al. [9] conducted an experimental study on the buckling behaviors of thin-walled GFRP unstiffened and stiffened cylindrical shells. Several specimens, unstiffened shells and stiffened shells with hexagonal, triangular, and lozenge grids with small skin thickness, were fabricated by a specially designed filament winding machine. All the specimens first experienced a general buckling failure mode as well as barreling before any visible damage could be observed. In addition, the local buckling mode on the skin of all specimens was recorded during the experiments. The shells with hexagonal and triangular grids exhibited maximum axial load while the unstiffened shells and the shells with lozenge grids showed somewhat less buckling capacity. On the other hand, when the specific buckling loads of the specimens were compared, it was found that the unstiffened shells had the highest specific buckling load followed by the stiffened shells with hexagonal and triangular grids. In the present work, 25 specimens (20 fully composite-stiffened shells and 5 unstiffened shells) were fabricated and tested under uniaxial compression loading. Two types of isogrid-stiffened shells with lozenge and triangular stiffeners were used. To obtain simply-supported boundary condition and avoid local boundary damages at the shell edges, epoxy rings were used at both ends of the shells. Axial load–displacement data were recorded in real-time during all experiments. The obtained results were then used to determine the maximum buckling load for each set of the specimens.

MATERIALS AND SPECIMEN PREPARATION

The specimens were fabricated from E-glass fiber and room-temperature-curing epoxy resin, using a specially designed filament winding machine. The nominal material properties are presented in Table 1, and the specifications of all specimens are given in Table 2. Figure 1 represents a schematic drawing of the grids in the

Table 1. Nominal material properties.

Material properties	Symbols	Unit	E-glass/Epoxy
Longitudinal modulus	E_{11}	GPa	36
Transverse modulus	E_{22}	GPa	5.8
Transverse modulus	E_{33}	GPa	5.8
Shear modulus	G_{12}	GPa	3.2
Poisson's ratio	ν_{12}	–	0.3
Density	ρ	kg/m^3	1.6

Table 2. Specification of different specimens.

Type of specimen	Name	Number of clockwise helical ribs	Number of counter-clockwise helical ribs	Number of hoop rings	Helical stiffeners winding angle (degree)	Shells winding angle (degree)	Approximate fiber volume fraction (%)
1	Unstiffened shells	–	–	–	–	65	56
2	Stiffened sells with lozenge grids	3	3	0	30	65	51
3	Stiffened sells with lozenge grids	4	4	0	30	65	51
4	Stiffened sells with lozenge grids	6	6	0	30	65	51
5	Stiffened sells with triangle grids	4	4	3	30	65	50

specimens used in this study. The cross-section area of all ribs was quadrangle with the area of $6 \times 6\,\text{mm}^2$. The specimens were characterized by an external diameter of 140 mm and an overall length of 314 mm, including two tabs provided at the top and bottom surfaces. These tabs were made from epoxy, and were used to attach specimens to the loading equipment.

Therefore, the actual length of shells was limited to the central section and measured 280 mm. The skin thickness of all specimens was 0.5 mm.

EXPERIMENTAL PROCEDURE

Experimental buckling tests were performed on the cylindrical shells under axial compression using a loading rig. For axial loading, an INSTRON 5500R test machine with a capacity of 200 KN in position control mode was used. Each specimen was tested under pure axial compression based on the ASTM D6641 standard with a loading rate of 1.3 mm/min. During the loading, the effective axial displacement and the compression load were recorded in real-time. All tests were continued until the first damage occurred, which happened when the load–displacement curve passed its maximum value. Therefore, the post-buckling and the mode shapes of buckling were not studied in this work. There

were two epoxy tabs provided at the top and bottom surfaces for attaching the specimens to the loading equipment [9]. This is an indication of the effect of boundary conditions on the general buckling behavior of the shells. Without these rings the general buckling in the specimen does not happen. Therefore, if studying the general buckling is the main objective, as it was for this work, it is necessary to use edge rings at both ends of the shells. Figure 2 shows the buckling mode shapes of specimens under uniaxial compression load.

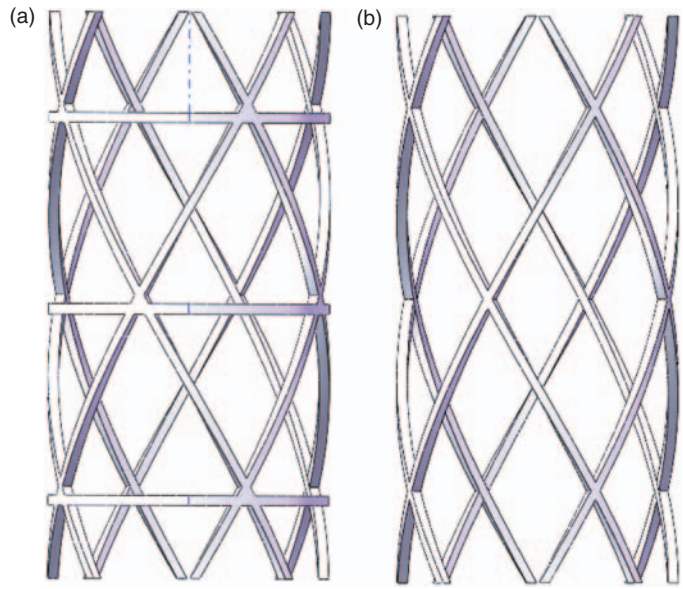

Figure 1. *Schematics of different grids: (a) triangle grids, (b) lozenge grids.*

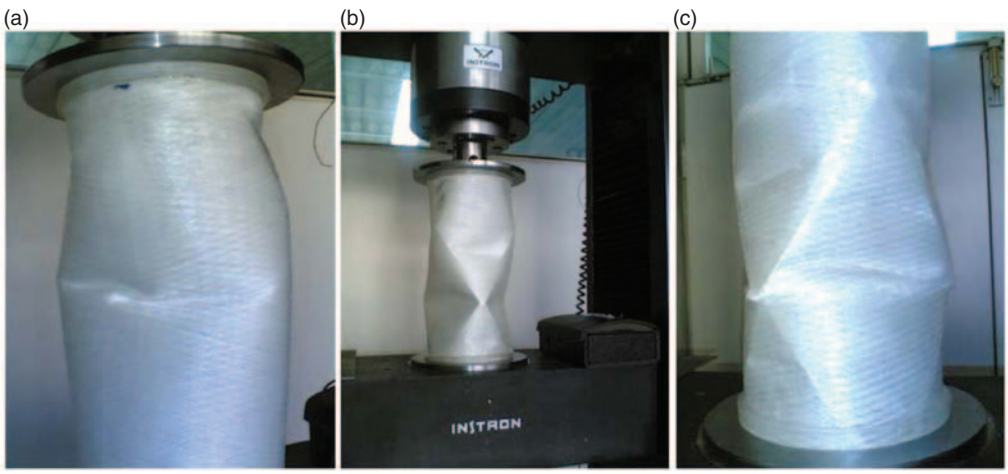

Figure 2. *Buckling mode shapes of three types of shells: (a) buckling of unstiffened shell, (b) buckling of stiffened shell with lozenge grids, (c) buckling of stiffened shell with triangle grids.*

RESULTS AND DISCUSSION

Figures 3 and 4 show the curves of load–displacement and specific load–displacement for types 1–5 specimens, respectively. The maximum buckling load for all cases occurred before the first skin damage was visually inspected for the type 1, 2, 3, 4, and 5 specimens as 5.061, 7.011, 10.793, 21.602, and 15.970 kN, respectively. Their corresponding maximum specific load, defined as load per mass, was 34.609, 30.831, 42.921, 63.250, and 49.202 kN/kg, respectively. Based on these observations, the maximum buckling load happens in type 4 grid-stiffened shells, followed by type 5, 3, 2, and 1 specimens.

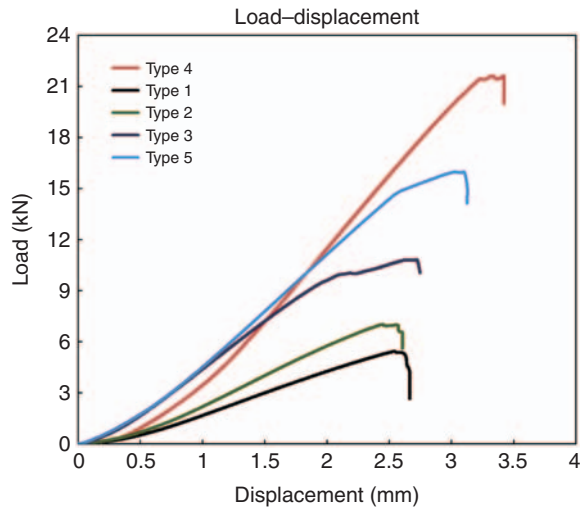

Figure 3. *Comparative chart for load–displacement curves of different specimens.*

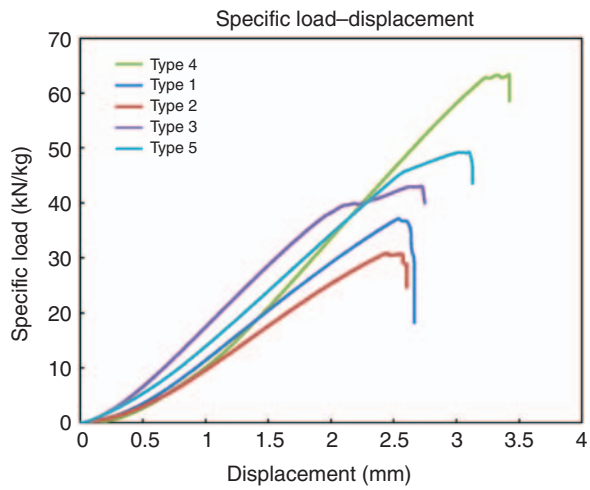

Figure 4. *Comparative chart for specific load–displacement curves of different specimens.*

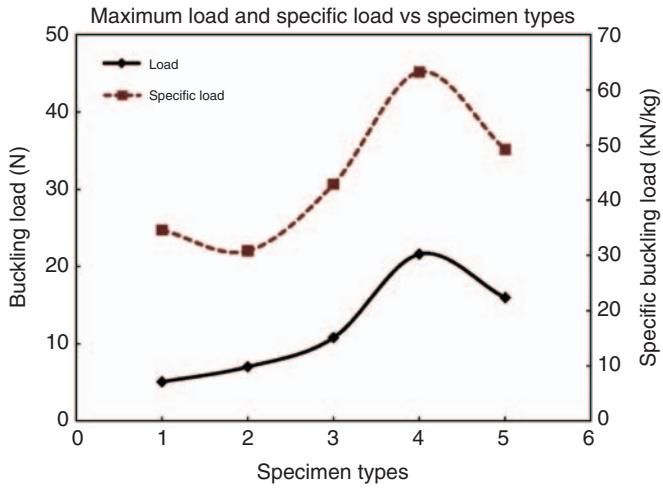

Figure 5. *Maximum buckling load and maximum specific load curves of different specimens.*

On the other hand, the maximum specific load was observed in type 4 of grid-stiffened shells, followed by type 5, 3, 1, and 2 specimens. It means that by adding six helical ribs to an unstiffened shell, its strength becomes weaker compared to that of the unstiffened one. Also, by increasing the number of stiffeners in the grid-stiffened shells the maximum buckling load increases, as shown clearly in Figure 5. This figure further shows that reinforcing unstiffened shells by lozenge grids (made of three clockwise and three counter-clockwise helical ribs, namely type 2 specimens) decreases the maximum specific load because of their additional mass. Yet by adding only one clockwise and one counter-clockwise helical rib to type 2 specimens, as it is the case in type 3 shells, the maximum buckling load as well as the maximum specific load in comparison to that of unstiffened shells increases. In this case, grid-stiffened shells demonstrate better performance than the unstiffened ones. By adding two clockwise and two counter-clockwise helical ribs in type 4 specimens, the maximum buckling load and the maximum specific load increased considerably in comparison to that of type 3 specimens. Similar to type 4 specimens, by adding three hoop rings to type 3 specimens and fabricating type 5 shells, the maximum buckling load and the maximum specific load increased in comparison to type 3 specimens. However, type 4 specimens had better performance than type 5 specimens. In addition, although type 4 shells had 5% more mass than type 5, the former specimens exhibited about 35.3% and 25.9% higher maximum bucking and maximum specific load, respectively, compared to the latter. On the other hand, the maximum displacement in type 4 specimens was 9.9% more than that of type 5 specimens. Therefore, in spite of minimum differences between the masses of the mentioned specimens, spiral ribs had a higher effect than hoop rings on axial buckling loading strength. Maximum displacement and maximum specific load for different specimens are shown in Figure 6. The maximum specific load and maximum displacement belong to type 4 specimens while the minimum value of these parameters was exhibited by type 2 specimens. As Figure 6 shows, by increasing the maximum displacement the maximum specific load also increases. Table 3 shows a summary of the experimental results.

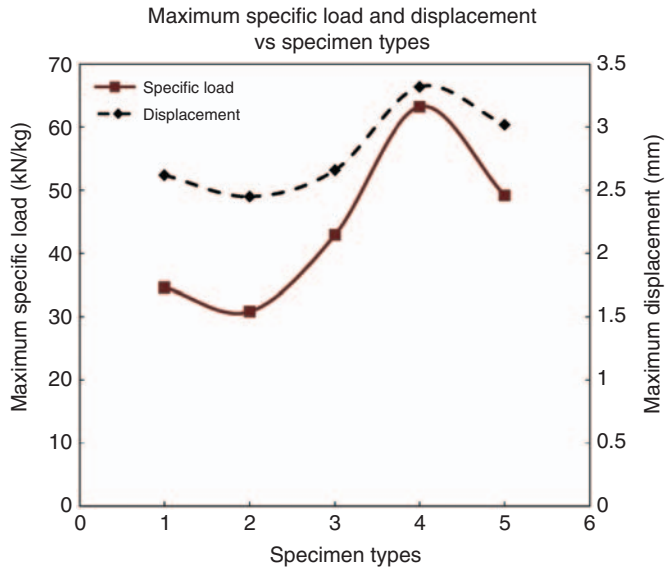

Figure 6. *Maximum displacement and maximum specific load curves of different specimens.*

Table 3. Buckling displacement, maximum buckling load, and maximum specific load of different specimens.

	Maximum displacement (mm)	Maximum buckling load (kN)	Mass (kg)	Maximum specific load (kN/kg)
Type 1	2.62	5.061	0.146	34.609
Type 2	2.45	7.011	0.227	30.831
Type 3	2.66	10.793	0.251	42.921
Type 4	3.32	21.602	0.341	63.250
Type 5	3.02	15.970	0.325	49.202

CONCLUSION

For high effectiveness of stiffeners on the strength of grid-stiffened composite shells there must be adequate stiffeners in the structures of shells. Obviously, by adding helical rib or hoop ring stiffeners to a structure, its maximum buckling load increases. However, the usage of these structures is in the aerospace industry, so the important parameter to study in the effectiveness of stiffeners is the specific buckling load. As shown in this study, by adding six helical ribs (three clockwise and three counter-clockwise helical ribs) to type 1 specimens, although the maximum buckling load increases the maximum specific load decreases significantly. On the other hand, the maximum specific load of type 3 specimens with eight helical ribs is higher than that of the unstiffened shells. It also shows that, in order to have a significant contribution on specific load, there must be an adequate number of helical ribs in the specimen's structure. For axial buckling loading, increasing the number of helical ribs is more effective than adding hoop rings and changing the

grids types. If the internal and/or external pressure loading are among the design factors, it seems that hoop rings are as effective as helical ribs on the strength of specimens. In this case, it is more important to select the best grid type. However, for pure axial loading, apparently the selection of lozenge grids with adequate helical ribs is the best choice.

REFERENCES

1. Baker, W. E. and Bennett, J. G. (1984). Experimental Investigation of Buckling of Nuclear Containment Like Cylindrical Geometries under Combined Shear and Bending, *Nuclear Engineering and Design*, **79**: 211–216.
2. Kim, T. D. (1999). Fabrication and Testing of Composite Isogrid Stiffened Cylinder, *Composite Structures*, **45**: 6–10.
3. Kim, T. D. (2000). Fabrication and Testing of Thin Composite Isogrid Stiffened Panel, *Composite Structures*, **49**: 21–25.
4. Meyer-Piening, H. R. (2001). Buckling Loads of CFRP Un-stiffened Composite Cylinders under Combined Axial and Torsion Loading–Experiments and Computations, *Composite Structures*, **53**: 427–435.
5. Bisagni, C. and Cordisco, P. (2003). An Experimental Investigation into the Buckling and Post-buckling of CFRP Shells under Combined Axial and Torsion Loading, *Composite Structures*, **60**: 391–402.
6. Wodesenbet, E. and Kidane, S. (2003). Optimization for Buckling Loads of Grid Stiffened Composite Panels, *Composite Structures*, **60**: 159–169.
7. Kidane, S. and Wodesenbet, E. (2003). Buckling Load Analysis of Grid Stiffened Composite Cylinders, *Composites: Part B*, **34**: 9–15.
8. Bisagni, C. and Cordisco, P. (2006). Post-buckling and Collapse Experiments of Stiffened Composite Cylindrical Shells Subjected to Axial Loading and Torque, *Composite Structures*, **73**: 138–149.
9. Yazdani, M., Rahimi, H., Khatibi, A. A. and Hamzeh, S. (2009). An Experimental Investigation into the Buckling of GFRP Stiffened Shells under Axial Loading, *Scientific Research and Essay*, **9**: 914–920.